Preprint from: Proceedings SPIE (4729) Signal Processing, Sensor Fusion, and Target Recognition XII, Orlando FL, April 2002.

Order Of Battle Change Detection, Fusion, And Tracking

Mark J. Carlotto, Mark A. Nebrich, and David Crary
Veridian Systems, 1400 Key Blvd., Suite 100, Arlington VA 22209

Abstract

The automatic detection of significant changes in imagery is important in a number of intelligence, surveillance, and reconnaissance (ISR) tasks. An automated capability known as the Order of Battle Change Fusion (OBCF) system is described for detecting, fusing, and tracking changes over time in multi-sensor imagery. OBCF uses multiple change detection algorithms to exploit different aspects of change in multi-sensor images, normalcy models that provide a physical basis for detecting change and estimating the performance of change detection algorithms, algorithm fusion to combine the results from multiple change detection algorithms in order to enhance and maintain performance over changing operating conditions, and stationary tracking to provide a seamless history of image changes over time across different sensing modalities. Preliminary experimental results using electro-optical (EO) and synthetic aperture radar (SAR) imagery are presented.

Introduction

After many decades of research, the automatic detection and assessment of significant change in imagery remains an important challenge. As the number of sensors and the flow of data from these sensors increases, and intelligence, surveillance and reconnaissance (ISR) requirements continue to expand in an ever changing world, the need to automatically perform certain kinds of routine tasks such as detecting and counting objects on the ground and monitoring changes in these objects over time is becoming increasingly important.

Under DARPA's Dynamic Database (DDB) program (Kessler 2001) a number of technical innovations were made that enable the development of an effective automated ISR change detection capability. These include the use of multiple change detection algorithms that exploit different aspects of change in multisensor imagery and the corresponding normalcy models which provide a physical basis for detecting change and estimating the performance of the change detection algorithms (Carlotto 1999, Hoogs and Mundy 2000, Tom et al 2000), algorithm fusion that combines the results from multiple change detection algorithms to enhance and maintain performance over changing operating conditions (Carlotto 2001), and stationary tracking to provide a seamless history of detected changes across sensing modality and time (Berlin et al 2000).

This paper describes an automated capability — the Order of Battle Change Fusion (OBCF) system — based on this technology for detecting, fusing, and tracking order of battle changes over time in multi-sensor imagery.

Order of Battle Change Fusion System

OBCF is a software system for detecting and monitoring change across multiple image sensors in time. It is divided into a processing component and a graphical user interface. The OBCF processing component consists of a bank of anomaly detectors which exploit different characteristics of manmade objects and changes. Spatial and temporal anomaly detectors exploit changes in the background over time. A scale-space anomaly detector identifies regions (possible manmade objects) that do not fit a fractal model for natural backgrounds over a range of spatial scales (resolutions). A set of detection surfaces are fused and possible changes in the background detected. Context maps can be used to eliminate false alarms in regions not likely to contain objects of interest. Detected regions are processed at the object level to further eliminate false alarms based on their size and shape. A Markov-based tracker associates and fuses detections from one or more sensor over time into tracks which define the state of possible manmade objects on the ground (appear, no change, or missing). This information is provided to the user in graphical and text summary form.

Space-Time Anomaly Detection

OBCF operates on a stack of geo-registered images acquired over a period of time. The most recent image is assumed to be at the top of the stack. Let a denote a pixel in this image, $\{b_n\}$ be the set of pixels which together with a constitute the k-th background type (Carlotto 2000), and $\{c_m\}$ be the set of pixel values at the same location as a but at previous times. The error in predicting a from the spatial average of the b_n (SAD prediction error) is

$$e_b = a - \frac{1}{N}\sum b_n \tag{1}$$

where the total number of pixels in the set $a \cup b_n$ is $N+1$. The SAD normalcy model assumes that under normal conditions (no targets present) all pixels in each set have similar values and deviations from the average may indicate the appearance of an object. The TAD prediction error is the error in predicting a from the temporal average of the c_n

$$e_c = a - \frac{1}{M}\sum c_m \,. \tag{2}$$

where M is the number of reference images. This normalcy model assumes that under normal conditions the value of a new pixel should be similar to the average of its previous values over time and that deviations from the average may indicate the appearance of an object.

Scale-Space Anomaly Detection

SAD and TAD detect changes between images. SSD operates on one image at a time and finds areas in the image that are anomalous (non-fractal) over scale. The idea of using fractals as models for detecting manmade objects in images was first proposed by Stein (1987). Earlier work by Mandelbrot and others (Pietgen et al 1992) showed that certain metric properties of natural terrain vary as a function of the scale of measurement (resolution) according to a power law. For example if $A(r)$ is the area of the terrain surface at resolution r,

$$A(r) = k r^{2-D} \tag{3}$$

where D is the fractal dimension and k is a constant of proportionality. As r decreases $A(r)$ increases at a rate that is related to the fractal dimension (roughness) of the surface. Kube and Pentland (1988) derived the conditions under which images of fractal surfaces are also fractal.

The object detection algorithm involves computing $A(r)$ over for a given set of resolutions $\{r_i\}$ using morphological operators, estimating the fractal dimension within a sliding window from the $A(r_i)$, and using the error between the fractal model and the $A(r_i)$ as a statistic for measuring the presence of manmade objects in the image. The fractal dimension estimate minimizes the mean-squared error

$$\varepsilon^2 = E\left[\log A(r_i) - \log k - (2 - D)\log r_i\right]^2. \quad (4)$$

SSD uses the root mean-squared error as a detection metric.

Table 1 OBCF Object-Level Features

Feature	Description
IDdet	Unique index
DTG	Date and time represented as YYYMMDD.HHMMSS
imageName	Input image
rank	Rank of detection in image (1 to N)
geoX	longitude or easting of centroid
geoY	latitude or northing of centroid
objectPresence	Change statistic normalized to 0-1
length	Length of oriented bounding rectangle in meters
width	Width of oriented bounding rectangle in meters
pose	Orientation of bounding rectangle (0-180 deg.)
area	Area of connected region in sq, meters
compactness	Ratio of the area to perimeter
intensityAve	Average value of input image within region
intensityStdev	Variation of input image within region
contrast	Contrast of input image along boundary
pixelLeft,pixelTop, pixelRight,pixelBottom	pixel coordinates of non-oriented bounding rectangle

Algorithm Fusion

OBCF achieves fusion gain from single as well as multiple sensors. Across sensors, fusion gain is achieved via stationary track processing as described below. Single sensor fusion is achieved by combining the outputs of SAD, TAD, and SSD each operating on the same input image. Previously we derived performance models for SAD and TAD individually and combined using AND fusion (Carlotto 2001). The performance gains (output SNR divided by input SNR) for SAD, TAD, and SAD+TAD can be approximated by:

$$Gain_{SAD} = \frac{1}{1-\beta}, \quad Gain_{TAD} = \frac{1}{1-\gamma}, \quad Gain_{SAD+TAD} = \frac{1}{1-\beta-\gamma+\alpha} \tag{5}$$

where β and γ are related to the cross-correlation of pixels in the spatial and temporally normalcy models, and α is the cross-correlation of pixels between the two models. In general, SAD and TAD performance improves as β and γ increase, and the fusion gain increases as α decreases. SSD is also fused by multiplying its change statistic with that of SAD and TAD.

Object-Level Processing

Before algorithm fusion can occur across sensors, fused single sensor detections are converted to an object-level representation. A set of object features are computed for each detection (Table 1).The object presence and rank are derived from the average value of the detection statistic squared over the region. Object presence is a key input to the tracking algorithm described in the next section. Size and shape are used to eliminate detections that are too large, or too small, or not compact enough to be man-made objects. Image features can be used to discriminate between bright and dark objects, and between low and high contrast changes. Other features are inherited by track and track state objects for the purpose of describing the geographic location and duration of changes.

Stationary Tracking

Detected changes across time and sensing modality are tracked and fused at the object-level. Stationary tracking associates new detections with existing tracks, and uses features of the detections to update the associated tracks. Tracks consist of a sequence of track state objects. Each track state object points to a detection. The logic for associating detections and tracks is if a detection is not associated with an existing unique track, create a new track; else, if an existing track is not associated with a unique detection, terminate the track; else, if an existing track is associated with one and only one detection, continue the track; else, if more than one detection is associated with a track, that track is terminated; else if more than one track is associated with a detection, both tracks are terminated. The last two conditions prevent ambiguity in associating multiple detections and multiple tracks.

As tracks evolve the current track state object in each active track is updated. Let $\Phi = \left[\phi_1 \cdots \phi_J\right]$ be the state vector of a track state object and $p(\phi_j, t)$ be the probability that the object is in state j at time t where. The state vector is updated using a first-order Markov model (Papoulis 1965)

$$p\left(\phi_j, t\right) = \sum_i P\left(\phi_j \middle| \phi_i\right) p\left(\phi_i, t-1\right) \tag{6}$$

where $P(\phi_j|\phi_i)$ is the probability that an object in state i at time $t-1$ transitions into state j at time t. In OBCF objects can be in one of four states: not present (NP), appear (A), no change (N), and missing (M). The transition probabilities depend on the object presence $0 \le d(t) \le 1$ of the detection that is associated with the track state object. The state update at each iteration multiplies the previous state vector by the current transition matrix:

$$\begin{bmatrix} p(\phi_{NP},t) \\ p(\phi_A,t) \\ p(\phi_N,t) \\ p(\phi_M,t) \end{bmatrix} = \begin{bmatrix} 1-d(t) & 0 & 0 & 0 \\ d(t) & 0 & 0 & d(t) \\ 0 & d(t) & d(t) & 0 \\ 0 & 1-d(t) & 1-d(t) & 1-d(t) \end{bmatrix} \begin{bmatrix} p(\phi_{NP},t-1) \\ p(\phi_A,t-1) \\ p(\phi_N,t-1) \\ p(\phi_M,t-1) \end{bmatrix} \tag{7}$$

to produce a new set of state probabilities. Prior to an object's appearance, $p(\phi_{NP}) = 1$. After an object disappears $p(\phi_M,t) \rightarrow 1$ as t increases. Fig. 1 shows the evolution of track state vectors for two cases. The first represents the sudden appearance, persistence, and disappearance of an object (a),

$$d(t) = \{0.0, 0.9, 0.9, 0.9, 0.9, 0.0\};$$

the second represents a more gradual appearance, persistence, and disappearance (b),

$$d(t) = \{0.0, 0.1, 0.5, 0.9, 0.5, 0.0\}.$$

The uncertainty in state is much less in the first case due to the higher object presence values.

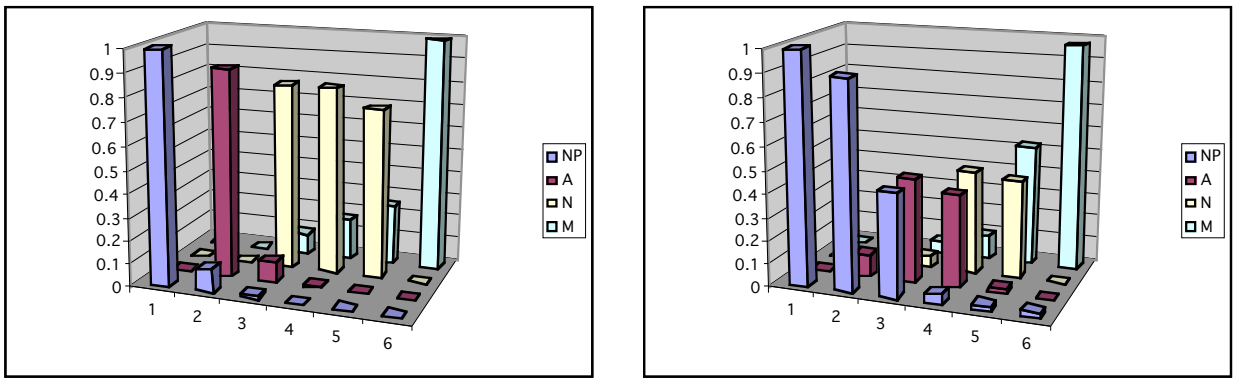

(a) (b)

Fig. 1 Examples showing evolution of track state vectors

False Alarm Elimination by Stationary Tracking

A major source of false alarms in SAR are glints caused by the coherent nature of the radar. A method used in OLCD (Tom et al 2000) to reduce false alarms is to group detections across different aspect angles into tracks. Changes which persist over a range of aspect angles give rise to tracks that are longer than those for false alarms due to their more transient behavior.

Veridian's unclassified Digital Collection System (DCS) was used to image a study area (DDB Site 13) in Florida using a 1 foot resolution Spotlight SAR. As the aircraft flies past a region of interest the sensor stares at and images a small area on the ground from different directions (look angles). Two DCS collections were made with and without vehicles (Fig. 2). The first set of images (a) was used for normalcy modeling and the second sequentially processed by OBCF to detect and track the vehicles.

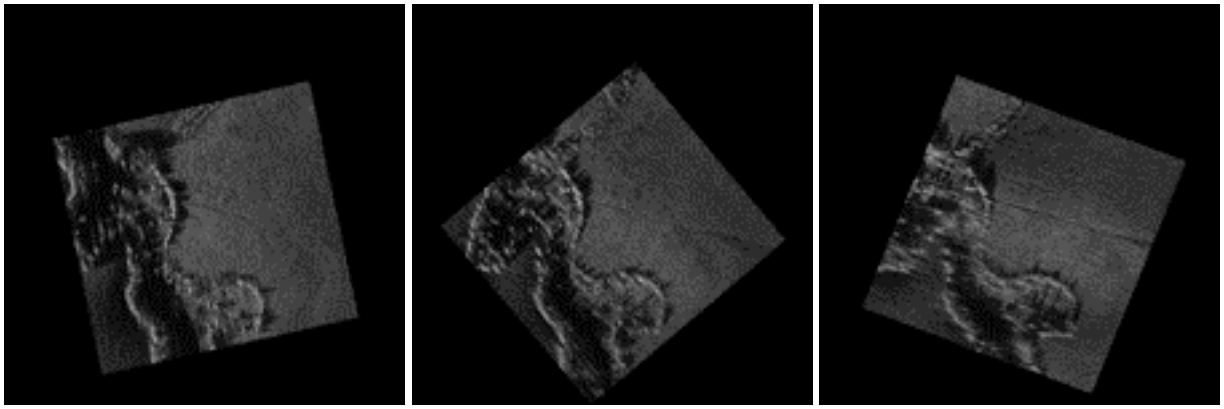

a) Three of five reference images without targets (aspect angles 78°, 50°, and 22°)

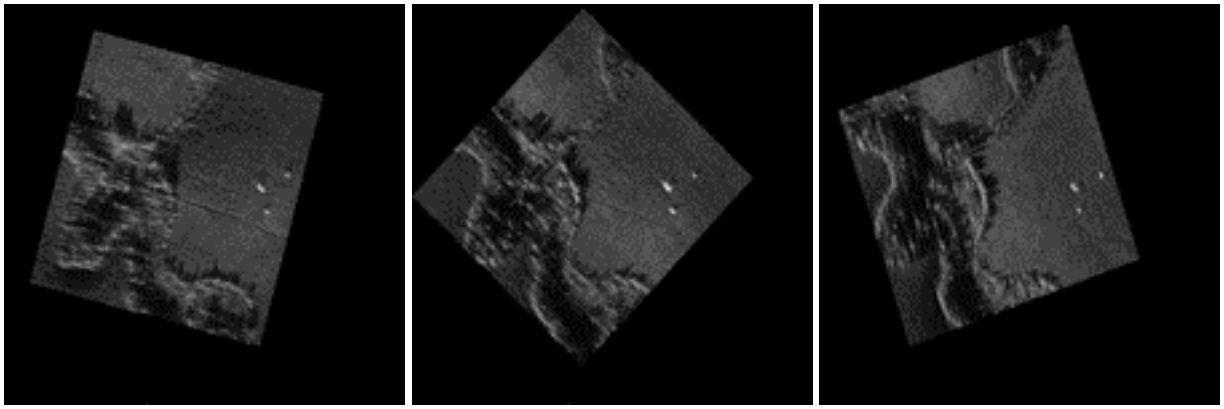

b) Three of five images with targets (aspect angles 13°, 41°, 69°)

Fig. 2 Spotlight SAR images

Five SAR images over an aspect angle range of 56° were processed sequentially using three images as reference images. Fig. 3a shows a portion of the Object History Summary (OHS) file created by OBCF as a by-product of the stationary tracking process. By filtering on track length all three objects can be detected with no false alarms (Fig. 3b).

trackID	trLength	objectPresence	score	geoX	geoY	area
0	5	0.997260	4.986300	567180.750000	3389919.250000	109.177505
2	5	0.951876	4.759381	567219.687500	3389902.000000	33.717339
1	5	0.950091	4.750453	567188.375000	3389954.500000	39.757030
52	4	0.817596	3.270382	566990.500000	3390051.500000	32.230568
4	4	0.674073	2.696291	566988.937500	3390027.250000	32.950802
57	4	0.644892	2.579570	567106.500000	3390049.750000	19.240593
86	3	0.858277	2.574832	567001.187500	3390112.750000	508.315186

a) Portion of Object History Summary (OHS) file with three tracks of length five highlighted.

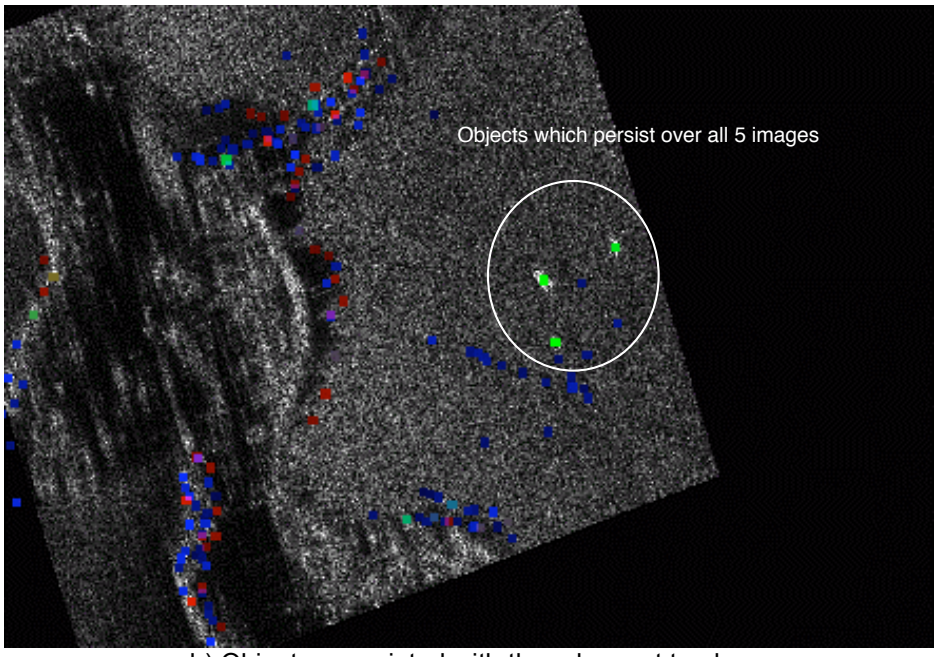

b) Objects associated with three longest tracks.

Fig. 3 SAR object tracking and false alarm reduction

Multisensor (SAR/EO) Change Detection and Tracking

In OBCF fusion across time occurs at the object level. Changes detected from different sensors can also be fused at the object level. Fig. 4 shows a portion of a multisensor SAR/EO sequence over the same area as above. The unclassified Army Night Vision and Electronic Sensors Directorate (NVESD) Dalsa CL-C8 Linescanner was used to collect electro-optical (EO) data over DDB Site 13. Three appearances are initially detected using EO (a). The next set of images are from the SAR. In (b), two of the objects persist, one leaves, and a number of other objects (including several false alarms) appear. The false alarms decorrelate in (c-f). Eight objects are present during this period of time with one false alarm created by a corner reflector. In the next EO image (g) all but two objects have disappeared. Finally, all of the objects are gone in the next set of SAR images (two of five are shown) in which all false alarms eventually decorrelate.

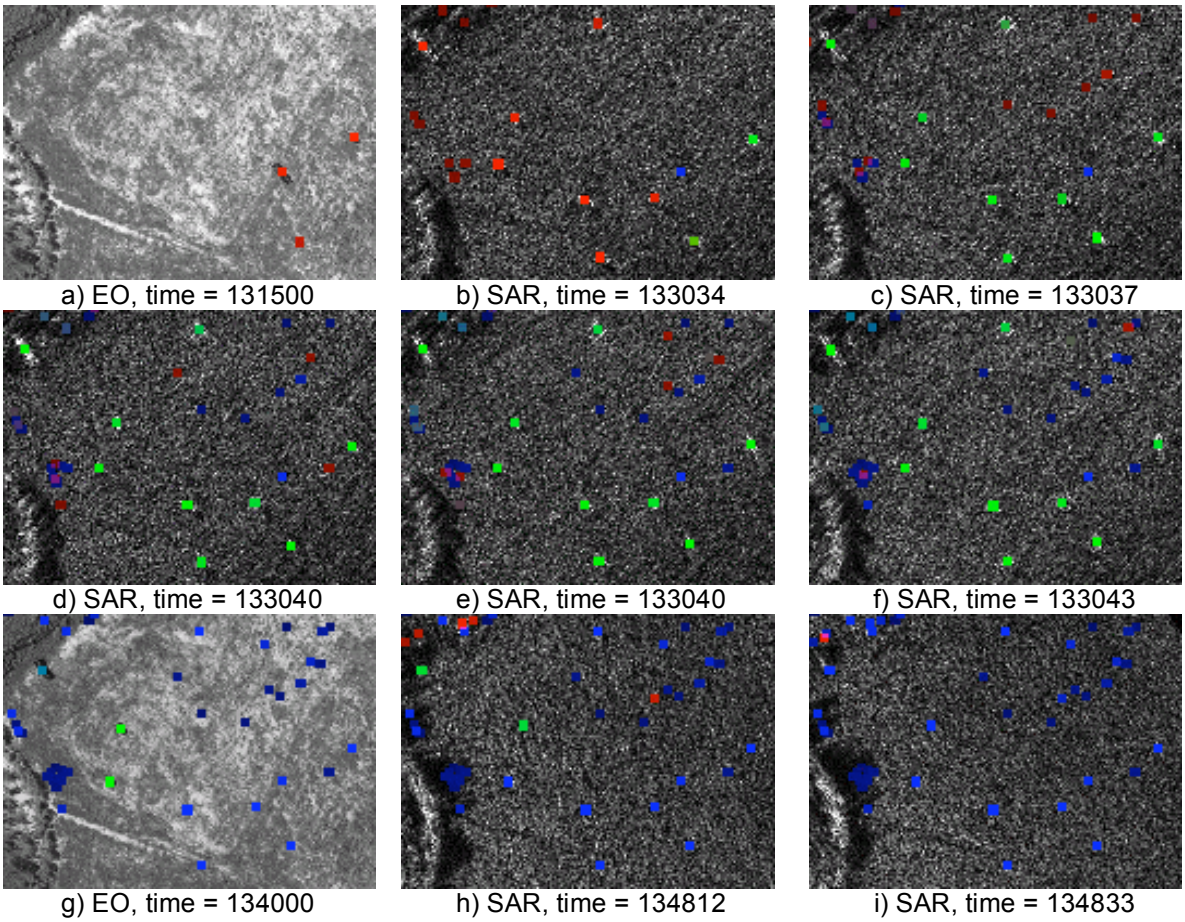

Fig. 4 Multisensor SAR/EO tracking example

Automatic Object Counting

OBCF uses information in the track state vector as a basis for counting objects in each image processed

$$O_A = \sum_{i \text{ objects}} \phi_{\mathrm{A}}^{\mathrm{i}}, \quad O_N = \sum_{i \text{ objects}} \phi_{\mathrm{N}}^{\mathrm{i}}, \quad O_M = \sum_{i \text{ objects}} \phi_{\mathrm{M}}^{\mathrm{i}} \tag{8}$$

where the total number of objects present in an image is $O_T = O_A + O_N$. Since the track state probability updates depend on the value of the object presence, the accuracy of the object counts depend on how accurately the object presence can be calibrated with actual object changes. We use a simple procedure that thresholds the object presence:

$$d' = \begin{cases} 1, & d > d_0 \\ 0, & \text{otherwise} \end{cases} \tag{9}$$

where the threshold is adjusted to make the counts in Eq. 8 agree with ground truth. If this is done for one image the threshold can be used to obtain counts for others in the sequence.

Two unclassified Ikonos images over an airfield in North Carolina were used to evaluate OBCF performance in counting aircraft. The first image acquired by Space Imaging on 3 May, 2000 contained 65 objects (aircraft and related pieces of equipment). For the purpose of this experiment a reference image was generated by "erasing" the objects. A second image acquired three months later on 10 August contained 80 objects. Although both images were acquired at the same local time, three months later the sun was lower in the sky and so shadows and image contrast are different. A context map used to restrict OBCF processing to the tarmac area.

Two counting experiments were performed: first with SAD+TAD fusion, and then with SAD+TAD+SSD fusion. The change statistic was calibrated using the number of objects in the May 3 image. The estimated counts (Table 2a) in the other images are accurate to within 15%. We repeated the experiment using SAD+TAD+SSD. Those object counts (Table 2b) are accurate to within 8%.

Table 2 Object counting results

Date	New	Persist	Missing	Total
5/3	65	0	0	65
	65	**0**	**0**	**65**
8/10	22	37	14	59
	30	**50**	**15**	**80**
After 8/10	0	0	87	0
	0	**0**	**80**	**0**

a) SAD+TAD estimated and actual (in

Date	New	Persist	Missing	Total
5/3	65	0	0	65
	65	**0**	**0**	**65**
8/10	32	46	13	78
	30	**50**	**15**	**80**
After 8/10	0	0	87	0
	0	**0**	**80**	**0**

a) SAD+TAD+SSD estimated and actual (in bold) counts

Summary

An automated capability known as OBCF was described for detecting, fusing, and tracking changes in multi-sensor imagery. OBCF uses two change detection algorithms (SAD and TAD) and a fractal-based object detection algorithm (SSD) to extract evidence of manmade objects and changes. OBCF can be extended to include additional change detection algorithms. Normalcy models provide a physical basis for detecting change and estimating the performance of the SAD and TAD algorithms. OBCF fuses the evidence provided by these algorithms to enhance and maintain detection performance over changing operating conditions. This information is integrated over time into stationary tracks that provide a seamless history of detected changes across sensing modality and time.

References

Mark Berlin, Mark Nebrich, and Martin Liggins, "Wide-Area SAR-EO Object Level Change Fusion Process for DDB," *2000 Meeting of the MSS National Symposium on Sensor and Data Fusion*, Kelly AFB, San Antonio TX, June 2000.

Mark J. Carlotto, "Image level change detection," *1999 IRIS National Symposium on Sensor and Data Fusion*, Laurel MD, 24-27 May 1999.

Mark Carlotto, "Nonlinear background estimation and change detection for wide area search," *Optical Engineering*, Vol. 39, No. 5, May 2000.

Mark Carlotto, "Detecting partially-obscured objects using multi-look SAR," *2000 Meeting of the MSS National Symposium on Sensor and Data Fusion*, Kelly AFB, San Antonio TX, June 2000.

Mark J. Carlotto, "A Signal-Level Fusion Model for Image-Based Change Detection in DARPA's Dynamic Database System," *SPIE Aerosense 2001 Conference on Signal Processing, Sensor Fusion, and Target Recognition X*, April 16-20, 2001 Orlando FL.

Anthony Hoogs and Joseph L. Mundy, " Information Fusion for EO Object Detection and Delineation," *2000 Meeting of the MSS National Symposium on Sensor and Data Fusion*, Kelly AFB, San Antonio TX, June 2000.

Otto Kessler, http://web-ext2.darpa.mil/tto/Programs/ddb.html, July 2000.

P. Kube and A. Pentland, On the imaging of fractal surfaces," I*EEE Trans. PAMI*, Vol 10, No 5, Sept. 1988.

A. Papoulis, *Probability, Random Variables and Stochastic Processes*, pp 381-382, McGraw-Hill, 1965.

H. Peitgen, H. Jurgens, and D. Saupe, *Chaos and Fractals*, Springer-Verlag, 1992.

M. C. Stein, "Fractal image models and object detection," *Society of Photo-optical Instrumentation Engineers,* Vol 845, pp 293-300, 1987.

Victor Tom, Helen Webb, and David Lefebvre, " Wide-Area SAR Object Level Change Detection," *2000 Meeting of the MSS National Symposium on Sensor and Data Fusion*, Kelly AFB, San Antonio TX, June 2000.